Signorino, G., Covaceuszach, S., Bozzi, M., Hubner, W., Mönkemöller, V., Konarev, P. V., Cassetta, A., Brancaccio, A., & Sciandra, F. (2018). A dystroglycan mutation (p.Cys667Phe) associated to muscle-eye-brain disease with multicystic leucodystrophy results in ER-retention of the mutant protein. *Human Mutation*, *39*(2), 266-280. https://doi.org/10.1002/humu.23370

Learn how to use

iPSC-derived Microglia to study Neurodegeneration

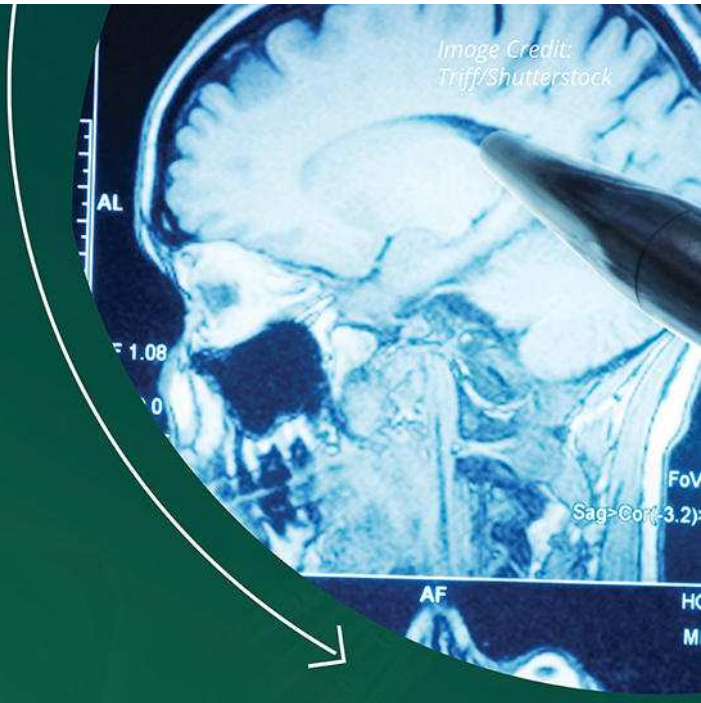

Webinar Details:
December 5, 2017
12:00 PM EST

Register Here

MilliporeSigma

CURRENT PROTOCOLS
A Wiley Brand

WILEY

307902

A dystroglycan mutation (p.Cys667Phe) associated to Muscle-Eye-Brain disease with multicystic leucodystrophy results in ER-retention of the mutant protein.

Giulia Signorino[1±], Sonia Covaceuszach[2±], Manuela Bozzi[1,3], Wolfgang Hubner[4], Viola Mönkemöller[4], Petr V. Konarev[5], Alberto Cassetta[2], Andrea Brancaccio[3,6*], Francesca Sciandra[3*]

[1] Istituto di Biochimica e Biochimica Clinica, Università Cattolica del Sacro Cuore, I-00168 Roma, Italy.
[2] Istituto di Cristallografia – CNR, Trieste Outstation, I-34149 Trieste, Italy.
[3] Istituto di Chimica del Riconoscimento Molecolare - CNR c/o Università Cattolica del Sacro Cuore, I-00168 Roma, Italy.
[4] Biomolecular Photonics, University of Bielefeld, 33615 Bielefeld, Germany.
[5] A.V. Shubnikov Institute of Crystallography of Federal Scientific Research Centre "Crystallography and Photonics" of Russian Academy of Sciences, Leninsky prospect 59, 119333 Moscow, Russia.
[6] School of Biochemistry, University of Bristol, Bristol BS8 1TD, United Kingdom.

[±] These authors contributed equally to this work

[*]Corresponding authors:

Francesca Sciandra, Istituto di Chimica del Riconoscimento Molecolare c/o Istituto di Biochimica e Biochimica Clinica, Università cattolica del Sacro Cuore, Largo F. Vito 1-00168 Roma-Italy
francesca.sciandra@icrm.cnr.it
Andrea Brancaccio, Istituto di Chimica del Riconoscimento Molecolare c/o Istituto di Biochimica e Biochimica Clinica, Università cattolica del Sacro Cuore, Largo F. Vito 1-00168 Roma-Italy
andrea.brancaccio@icrm.cnr.it

Grant: Association Française contre les Myopathies (n.20009)

Abstract

Dystroglycan (DG) is a cell adhesion complex composed by two subunits, the highly glycosylated α-DG and the transmembrane β-DG. In skeletal muscle, DG is involved in dystroglycanopathies, a group of heterogeneous muscular dystrophies characterized by a reduced glycosylation of α-DG. The genes mutated in secondary dystroglycanopathies are involved in the synthesis of O-mannosyl glycans and in the O-mannosylation pathway of α-DG. Mutations in the DG gene (*DAG1*), causing primary dystroglycanopathies, destabilize the α-DG *core protein* influencing its binding to modifying enzymes.

This article has been accepted for publication and undergone full peer review but has not been through the copyediting, typesetting, pagination and proofreading process, which may lead to differences between this version and the Version of Record. Please cite this article as doi: 10.1002/humu.23370.

Recently, a homozygous mutation (p.Cys699Phe) hitting the β-DG ectodomain has been identified in a patient affected by Muscle-Eye-Brain disease with multicystic leucodystrophy, suggesting that other mechanisms than hypoglycosylation of α-DG could be implicated in dystroglycanopathies. Herein, we have characterized the DG murine mutant counterpart by transfection in cellular systems and high-resolution microscopy. We observed that the mutation alters the DG processing leading to retention of its uncleaved precursor in the endoplasmic reticulum. Accordingly, small-angle X-ray scattering (SAXS) data, corroborated by biochemical and biophysical experiments, revealed that the mutation provokes an alteration in the β-DG ectodomain overall folding, resulting in disulfide-associated oligomerization. Our data provide the first evidence of a novel intracellular mechanism, featuring an anomalous endoplasmic reticulum-retention, underlying dystroglycanopathy.

Keywords: dystroglycan, dystroglycanopathy, multicystic leukodystrophy, site-directed mutagenesis, confocal microscopy, super resolution microscopy, endoplasmic-reticulum retention, SAXS.

Introduction

Dystroglycan (DG) is an adhesion complex expressed in skeletal and cardiac muscle as well as in epithelial tissue and in central and peripheral nervous systems (Bozzi et al., 2009). DG is composed by two subunits, α- and β-DG, that interact non-covalently to form a bridge between the extracellular matrix and the actin cytoskeleton. In fact, the α-subunit is a highly glycosylated extracellular protein that binds laminin-globular (LG) domain-containing extracellular matrix proteins such as laminins, perlecan, agrin, and neurexins, while β-DG is a transmembrane protein that interacts with the actin cytoskeleton (Moore and Winder, 2012). α- and β-DG arise from a post-translational cleavage of a single precursor encoded by the *DAG1* gene (MIM# 128239) (Ibraghimov-Beskrovnaya et al., 1992). α-DG is formed by two globular domains, the N-terminal and the C-terminal, separated by a mucin-like region rich in O-linked glycans (Brancaccio et al., 1997). The extensive O-linked glycosylated moieties belonging to the central domain of α-DG mediate the interaction between the α-DG and the LG domains of laminins and other ligands. In particular, a specific phospho-glycan has been recently identified and characterized as the functional glycan unit of α-DG (Willer et al., 2014; Yoshida-Moriguchi and Campbell, 2015; Kanagawa et al., 2016). This repeated disaccharide unit have been shown to bind an epitope on the LG4 domain of laminin-α2 and form a coordination with a calcium atom (Briggs et al., 2016). The N-terminal domain of α-DG is shed immediately after the interaction with LARGE, the enzyme which is crucially involved in the synthesis of the aforementioned repeated units, (Kanagawa et al., 2004) whilst its C-terminus interacts with the extracellular domain of β-DG (Sciandra et al.,

2001). The N-terminal ectodomain of β-DG is a natively unfolded protein characterized by a high conformational plasticity that enables β-DG to transduce extracellular signals inside the cells (Bozzi et al., 2003). Indeed, the β-DG cytoplasmatic domain binds to several signalling and adaptor proteins and it is able to modulate the actin-cytoskeleton architecture in response to external stimuli (Colognato et al., 1999; Russo et al., 2000; Spence et al., 2004; Bozzi et al., 2009). Recently, it was shown that the binding between agrin and α-DG promotes the disassembly of the β-DG scaffold which inhibits the Hippo pathway in the adult heart thus stimulating the cardiomyocytes proliferation (Bassat et al., 2017; Morikawa et al., 2017).

In skeletal muscle, DG is the central component of the dystrophin-glycoprotein complex (DGC), a group of peripheral and integral membrane proteins that ensures muscle stability during multiple contraction and relaxation cycles (Bozzi et al., 2009). Mutations in any one of the DGC members compromise the stability of the entire complex, leading to the development of different forms of muscular dystrophies. Duchenne and Becker muscular dystrophies (DMD MIM# 310200 and BMD MIM# 300376) are caused by different mutations in the dystrophin gene. Mutations of sarcoglycans are associated with autosomal recessive limb-girdle muscular dystrophies (LGMD), while mutations in the laminin-α2 chain gene (*LAMA2*, MIM# 156225) are linked to merosin-deficient congenital muscular dystrophy (MCMD1, MIM# 607855). In addition, a number of genetically heterogeneous neuromuscular disorders, collectively known as secondary dystroglycanopathies, are caused by mutations in several genes that are involved in the intricate O-mannosyl glycosylation of α-DG (Yoshida-Monriguchi et al., 2015). Possibly, one common feature of secondary dystroglycanopathies is the expression of a hypoglycosylated form of α-DG, whose ability to bind laminin and the extracellular

matrix is markedly reduced (Michele et al., 2002). These disorders include various forms of LGMDs and of severe congenital muscular dystrophies (CMDs), with or without additional ocular and brain abnormalities. The CMDs include Fukuyama CMD (MDDGA4, MIM# 253800 and MDDGB4 MIM# 613152), muscle-eye-brain disease (MDDAGA3, MIM# 253280 and MDDGB3 MIM# 613151) and Walker-Warburg syndrome (MDDGA1, MIM# 236670, MDDGA2, MIM# 613150, MDDGB1, MIM# 613155 and MDDGB2, MIM # 613156).

Only four cases of primary dystroglycanopathy, directly affecting *DAG1* gene, have been reported so far. A homozygous frameshift mutation in the *DAG1* (NM_001165928.3, c.743delC, p.Ala248Glufs), which results in a premature stop codon and in a complete absence of both α- and β-DG, was found in five patients from a consanguineous family who were affected by severe CMD with brain and eye anomalies and died after birth (Riemersma et al., 2015). A second case is a patient affected by mild LGMD accompanied by cognitive impairment (MDDGC9, MIM# 613818) (Hara et al., 2011). A homozygous missense mutation (c.575C>T) causes a threonine-to-methionine substitution at the amino acid residue 192 (p.Thr192Met) within the N-terminal domain of α-DG. The mutation affects the overall flexibility of the N-terminal domain of α-DG and inhibits the interaction between LARGE and α-DG preventing the functional modification of the mucin-like domain DG (Hara et al., 2011; Bozzi et al., 2015; Covaceuszach et al., 2017a). In addition, hypoglycosylated α-DG influences the β-DG functional properties reducing its ability to form actin clusters (Palmieri et al., 2017). In the third case of a primary dystroglycanopathy, compound heterozygous mutations in *DAG1* (c.220G>A and c.331G>A) lead to valine-to-isoleucine (p.Val74Ile) and to aspartic-to-asparagine (p.Asp111Asn) substitutions, respectively (Dong et al., 2015)). The two missense

mutations are located within the N-terminal region of α-DG affecting both the flexibility in solution and the glycosylation of the α-subunit and its laminin binding (Covaceuszach et al., 2017b). The patients had asymptomatic hyperCKemia and developed a mild muscular dystrophy with no central nervous system involvement.

The fourth case of primary dystroglycanopathy was found in two siblings affected by severe CMD with central nervous system anomalies (MIM# 616538) and multicystic leukodystrophy (Geis et al., 2013). A homozygous missense mutation (c.2006G>T) results in a cysteine-to-phenylalanine substitution at residue 669 (p.Cys669Phe) in the extracellular domain of β-DG and it was predicted to disrupt the intramolecular disulfide bridge with Cys713 thus altering the tertiary structure of the β-DG ectodomain (Deyst et al., 1995; Watanabe et al., 2007; Sciandra et al., 2012). Moreover, based on a partial immunohistochemical analysis of muscle biopsies it seemed that α-DG was hypoglycosylated, whilst laminin was still deposited around the skeletal muscle fibers (Geis et al., 2013). However, no extensive biochemical characterization of the mutant DG has been reported yet. Currently, it is still not clear how the p.Cys669Phe mutation affects the DG expression and maturation. In particular, it is not known whether the mutation affects the α-DG post-translational modifications or it perturbs the association of α-DG with the other components of the DGC.

In this work, we expressed the murine counterpart (p.Cys667Phe) of the p.Cys669Phe DG in a heterologous cell expression system and we showed that the processing of the mutated DG is inhibited and that the mutant protein is mostly engulfed in the endoplasmic reticulum. Moreover, by biochemical, biophysical and structural characterization we showed that the mutant ectodomain of β-DG displays an altered folding and leads to the

formation of high molecular weights disulfide-associated homo-oligomers, suggesting a novel intracellular mechanism for dystroglycanopathies.

Methods

Dna manipulation

The single point mutation p.Cys667Phe was introduced into the murine DG (BC007150.1) construct containing a myc-tag inserted within the C-terminus of α-DG and cloned in pEGFP vector (Morlacchi et al., 2012) using the Quick Change site-directed mutagenesis kit (Stratagene, USA) and the following primers:

Forward 5'-CCCTTGGAGCCCTTCCCCAAGGAGCAG-3'

Reverse 5'-CTGCTCCTTGGGGAAGGGCTCCAAGGG-3'

An expression bacterial vector containing the β-DG ectodomanin (spanning the amino acids 654-750) in frame with an N-terminal 6xHis tag, the thioredoxin protein, and a thrombin cleavage site (Sciandra et al., 2001), was used as template to introduce p.Cys667Phe mutation using the Quick Change site-directed mutagenesis kit (Stratagene) and the primers described above.

The constructs were verified by automated sequencing.

Cell culture, transfection and Western blot

Ebna-293 cells were grown in DMEM supplemented with 10% fetal calf serum and antibiotics. The cells at 80% of confluence were transiently transfected with 20μg of wild-type or p.Cys667Phe constructs using the calcium phosphate method as described

elsewhere (Morlacchi et al., 2012). 48 h after transfection, cells were harvested and lysated with lysis buffer (PBS containing 1% TritonX-100 and proteinase inhibitors) for 1h. After centrifugation at 10.000 rpm, the cleared protein extracts were quantified and 10 or 20 μg of total protein extracts were resolved on a 4-15 % SDS-PAGE (Bio-Rad Laboratories, USA). Protein were then transferred to nitrocellulose and probed with different primary antibodies: anti-myc HRP (1:5000) (Miltenyi, Germany) and a monoclonal anti-β 43-DAG (1:50) (Novacastra, UK). The reactive products were revealed using the luminol-based ECL system (Pierce, USA). To analyze the effect of proteasome inhibition, 36h after the transfection Ebna-293 cells were incubated with 20 μM of lactacystin (Sigma-Aldrich, USA) dilute in water. After 16h the cells were harvested and analysed by Western-blot. Quantification of DG^{WT} and DG^{C667F} precursor, normalized to tubulin, was performed using ImageJ software (National Institutes of Health; Bethesda, MD). Two-tailed Student's t-tests was used for the statistical analysis of protein levels.

sWGL-enrichment assay

20 μg of total protein extracts of cells expressing DG^{WT} and DG^{C667F} were incubated with succinylated Wheat Germ Lectin (sWGL) Sepharose 6MB (Amersham, USA) and equilibrated in lysis buffer overnight at 4°C. After extensive washing with washing buffer (WB) (PBS containing 1% Triton X-100), bound glycoproteins were eluted in WB containing 300 mM N-acetylglucosamine and analysed by Western blot.

Cell surface protein isolation kit

Membrane proteins were isolated using the Cell Surface Protein Isolation kit (ThermoFisher, USA), following the manufacturer instructions. Briefly, transiently transfected Ebna-293 cells were labelled with Sulfo-NHS-SS-Biotin solution, for 30 minutes at 4°C. After adding quenching solution and washing with TBS, cells were

harvested and lysed with lysis buffer. Equal amounts of cell lysates were used to isolate labelled membrane proteins with NeutrAvidin Agarose beads. Biotinylated proteins were then eluted with 50 µl of sample buffer containing DTT. Samples were analysed by Western blot. Quantification of DG wild-type and p.Cys667Phe precursor, normalized to endogenous DG, was performed using ImageJ software (National Institutes of Health; Bethesda, MD). Two-tailed Student's t-tests was used for the statistical analysis of protein levels.

Immunofluorescence and microscope analysis

Ebna-293 transiently transfected cells were fixed with 4% paraformaldehyde for 20 minutes at room temperature. Non-specific sites were blocked with 1% BSA in PBS or in PBS containing 0.2% TritonX-100 that is able to permeabilize the cells. Cells were incubated with the anti-myc antibody polyclonal (1:100, ThermoFisher, USA) and/or anti Erp-57 monoclonal antibody (1:100, AbCam, UK) for 1h. Cells were washed with PBS and then incubated with an anti-rabbit or anti-mouse secondary antibody conjugated with rhodamine (1:100, ThermoFisher, USA) and imaged with a confocal laser scanning system (A1+, Nikon, Japan). Laser excitation at 488 nm was followed by an excitation at 583 nm to collect emission signals from GFP and rhodamine, respectively. Super-resolution 3D Structured Illumination Microscopy (3D-SIM) was performed as previously described on an OMX v4 (GE Healthcare, UK) (Bozzi et al., 2015). U2OS cells were transiently transfected with the appropriate plasmids and observed at 24°C live in order to preserve the ER structure.

Expression and purification of the wild-type and C667F β-DG recombinant ectodomain

The wild-type and p.Cys667Phe β-DG ectodomains were expressed in the E. coli BL21 codon plus strain and purified using nickel nitrilotriacetate (Ni-NTA) affinity chromatography (Novagen, Germany). The eluted thioredoxin fusion proteins, previously dialyzed in a buffer containing 20 mM Tris-HCl, 0.15 M NaCl, 2.5 mM CaCl2, pH 8.4, were incubated with thrombin from human plasma (Sigma-Aldrich, USA) for 4 h at room temperature. The thioredoxin fusion partner was then removed with a second Ni-NTA affinity chromatography step. The purity of the isolated β-DG ectodomains were checked by 12% SDS PAGE, stained with Coomassie Brilliant Blue R-250 dye.

Analytical gel filtration

Analytical gel filtration was performed on a Superdex 75 10/300 column (GE Healthcare, UK), pre-equilibrated and eluted with 20 mM Tris, 150 mM NaCl pH 7.5: the concentration of both injected sample was 0.25 mg/ml in 20 mM Tris-HCl pH 7.5. Fraction corresponding to the main peaks have been checked by 15% SDS PAGE and Coomassie staining. The column was previously calibrated with Apoprotin (6.5 kDa), ribonuclease A (13.7 kDa), ovalbumin (43 kDa) and bovine serum albumin (66 kDa) in 20 mM Tris, 150 mM NaCl pH 7.5 and the apparent Molecular Weights (MMs) of the samples were estimated using the column calibration against these standard protein.

Differential Scanning Fluorimetry (DSF)

DSF measurements were carried out using a CFX96 Touch Biorad Real-Time PCR system (Bio-Rad Laboratories, USA) with λ_{ex} = 470-505nm, λ_{em} = 540-700 nm. The protein stocks contained 20 mM Tris pH 7.5 and were mixed at final concentration of 1 mg/ mL with 90× SYPRO Orange (Sigma-Aldrich, USA). Temperature increments of 0.2

°C/min and a temperature range of 20-90°C were used. Experiments were performed in triplicate.

Limited proteolysis

β-DG wild-type and p.Cys667Phe mutant recombinant proteins were subjected to limited proteolysis at 37°C at a final concentration of 30 μM in 20 mM Tris pH 7.5 buffer. A panel of five proteases from Proti-Ace kits (Hampton Research, USA), i.e. actinase, elastase, subtilysin, thermolysin and trypsin were tested at a final concentration of 2 μg/ml. The reactions were stopped after 1, 5, 10, 20, 40 and 60 min by adding SDS sample buffer to aliquots of the reaction mixtures. The samples were analyzed by performing 15% SDS-PAGE and Coomassie staining.

Small-angle X-ray scattering measures and data processing

SAXS data for β-DG wild-type and p.Cys667Phe mutant proteins were collected on the P12 beamline EMBL SAXS-WAXS at PETRAIII/DESY (Blanchet et al., 2015) (Hamburg, Germany) as 20x 0.05 s exposure times using a Pilatus 2M (Dectris, Switzerland) pixel array X-ray detector, sample-detector distance 3.00 m, wavelength 1.24 Å. Measurements were carried out at 5 different concentrations (the ranges are reported in Table S1) in 20 mM Tris pH 7.5, in presence and in absence of 10 mM DTT. No radiation damage was detected comparing scattering profiles for the collected frames.

Processing steps were performed with PRIMUS (Konarev et al., 2003) from the ATSAS 2.6.0 program package (Petoukhov et al., 2012). After normalization to the intensity of the transmitted beam and averaging of the frames for each sample, the buffer's contribution was subtracted to the scattering. As some inter-particle attractive interactions were observed at high protein concentration in all the samples, the low *s*-data of diluted

samples (0.9 and 1.4 mg/ml for wild-type and p.Cys667Phe respectively), where inter-particle interactions are negligible, were merged with the high *s*-data of the concentrated samples (3.9 and 5.3 mg/ml respectively).

The forward scattering I(0) and the radius of gyration R_g were evaluated using the Guinier approximation (Guinier, 1939) assuming that at very small angles ($s < 1.3/R_g$) the intensity is represented as

$$I(s) = I(0) * e^{\frac{-(s*R_g)^2}{3}}.$$

Pair distance distribution functions of the particles P(r) and the maximum sizes D_{max} were computed using GNOM (Svergun, 1992). MMswere estimated by comparison of the calculated forward scattering I(0) of the samples with that of the standard solution of bovine serum albumin (MM 66kDa). The excluded volume of the hydrated protein molecule (V_p) was calculated using the Porod approximation (Porod, 1982):

$$V_p = \frac{2\pi^2 I(0)}{\int I_{exp}(s) s^2 ds}.$$

Results

p.Cys667Phe mutation inhibits processing and membrane targeting of dystroglycan

To better understand the influence of the mutation p.Cys669Phe on the expression and maturation of DG, by site-directed mutagenesis we imported the murine counterpart mutation (p.Cys667Phe) into the sequence of DG cloned in a pEGFP vector that was subsequently used to transfect Ebna-293 cells. The same construct also contained a myc tag inserted within the C-terminal region of α-DG (Morlacchi et al., 2012).

Western blot analysis of total protein extracts using a commercial anti-β-DG antibody showed that the mutation p.Cys667Phe inhibits post-translational cleavage of the DG precursor. In fact, p.Cys667Phe mutant migrated as a single 160 kDa band, similarly to the previously characterized DG mutant carrying the mutation p.Ser652Ala at the α/β-DG cleavage site that was used as a control (Fig.1A) (Jayasinha et al., 2003; Esapa et al., 2003; Akhavan et al., 2008). The same total protein extracts were incubated with agarose-immobilized sWGL (succinylated Wheat Germ Lectin) that specifically binds N-acetylglucosamine residues (Fig. 1B). The mutant DG precursor was pulled down by this procedure, as confirmed by Western blot, suggesting the presence of N-acetylglucosamine moieties within the uncleaved protein (Fig. 1B). However, the low affinity displayed by the IIH6 antibody for α-DG expressed in Ebna-293 cells, prevented us to verify the presence within the p.Cys667Phe DG precursor of the glycan moiety responsible for α-DG binding to laminin which is specifically targeted by IIH6 (Palmieri et al., 2015).

By immunofluorescence staining of non-permeabilized transfected cells, we showed that the wild-type DG was primarily localized at the plasma-membrane, either following the EGFP signal reporting β-DG localization or the anti-myc reporting α-DG localization (Fig. 2A). On the other hand, only a limited amount of the p.Cys667Phe mutant was detectable at the plasma membrane (Fig. 2A). However, immunofluorescence of detergent-permeabilized transfected cells showed that p.Cys667Phe mutant was mainly detected intracellularly and displaying a reticular pattern (Fig. 2A). DG carrying the mutation p.Cys667Phe largely co-localized with Erp57, an ER resident protein (Fig. 2B), suggesting that the mutant is retained in the ER. The same result was obtained with a different cell line, U2OS human bone osteosarcoma cell line, strongly pointing out that

the observed effect depends on the p.Cys667Phe mutation irrespective of the cellular type under analysis (Fig. 3, Supp. Fig. S1).

To further verify that we indeed observed a strong intracellular retention of p.Cys667Phe mutant, as suggested by immunofluorescence, cell surface biotinylation was used to establish whether the mutant was trafficked to the plasma membrane of transfected Ebna-293 cells. Indeed, we confirmed that whilst wild-type DG was recovered in the biotinylated fraction, only a minor fraction of p.Cys667Phe mutant was targeted to the plasma membrane (Fig. 4).

p.Cys667Phe mutant is targeted by the ubiquitin-mediated degradation systems

It was predicted that mutation of Cys667 would disrupt an intramolecular disulfide bond important for folding and correct processing of the precursor DG (Deyst et al., 1995; Watanabe et al., 2007; Sciandra et al., 2012). Typically, misfolded proteins undergo degradation *via* the ubiquitin-proteasome system (Cohen-Kaplan et al., 2016). To test whether p.Cys667Phe mutant is targeted to the proteasome, we treated transfected cells with the proteasome inhibitor lactacystin. Interestingly, whilst the incubation with lactacystin increased the level of wild-type DG, the level of p.Cys667Phe mutant was further reduced (Fig. 5A).

In addition, total extracts of transfected cells treated with lactacystin were immunoprecipitated with anti-GFP conjugated agarose beads and the resulting fractions were analysed by Western blot using an anti-ubiquitin antibody. The proteasome inhibition of transfected cells allowed to observe the presence of bands corresponding to the mutant DG conjugated to poly-ubiquitin moieties, otherwise rapidly degraded (Fig. 5B). The detection of poly-ubiquitinated wild-type β-DG suggested that also a fraction of

the wild-type protein is targeted to be destroyed within the proteasome, probably due to the strong overexpression of the construct which is somehow overcrowding the ER and the cytosol (Fig. 5B).

Overall, these data indicate that the mutant DG engulfed in the ER is intercepted by its resident quality-control system and accordingly is targeted to degradation through the ubiquitin-mediated degradation pathway.

Pathological missense p.Cys667Phe mutation induces disulfide-associated β-DG oligomerization.

Previously, we have expressed and characterized the recombinant ectodomain of β-DG showing that it is a largely unstructured protein (Di Stasio et al., 1999; Boffi et al., 2001; Bozzi et al., 2003). Therefore, we investigated the potential effect of the p.Cys667Phe mutation on the overall folding of the recombinant extracellular domain of β-DG by a series of biochemical approaches (Fig. 6 and 7).

Analysis of wild-type β-DG by SDS-PAGE (Fig. 6A) showed that boiling protein samples with SDS under non-reducing conditions resulted in a single band corresponding to monomers. On the contrary, the β-DG carrying the p.Cys667Phe mutation gave two major bands corresponding to a mixture of dimers and monomers. Boiling samples with DTT and SDS reduced all the two preparations to the molecular mass expected for monomeric β-DG suggesting that the mutant β-DG dimers observed under non-reducing conditions were covalently linked through an inter-molecular disulfide bond involving Cys711. This result was also confirmed by native gels under non-reducing and reducing conditions (data not shown).

A more complex scenario was revealed by analytical gel-filtration, Dynamic Light Scattering (DLS) and Small Angle X-Rays scattering (SAXS) experiments.

The elution patterns obtained for wild-type and p.Cys667Phe β-DG (Fig. 6B) showed striking differences. In details wild-type β-DG resulted in a single main peak corresponding to an apparent molecular mass of a dimeric molecule. In contrast, the p.Cys667Phe mutation resulted in a complex elution profile, yielding a major fraction (50%) of higher oligomers (eluting in the void volume), two peaks corresponding to lower oligomers, i.e. tetramers (10%) and trimers (5%), and a final peak (35%) corresponding to a monomeric fraction.

These differences in the oligomerization states between the wild-type and the mutant β-DG were further corroborated by DLS (see Supplemental Information) and by SAXS measurements of the two protein samples (see Supp. Table S1). The scattered intensity is sensitive to the size and shape of the protein in solution; therefore, from the analysis of such plots hypothesis on the conformation of the molecule can be made (Receveur-Brechot et al., 2006). The derived experimental scattering patterns displayed no systematic changes with the solute concentration, demonstrating no change in association state of wild-type and mutant β-DG with concentration, in accordance with DSL measurements. Even if both samples showed a small level of aggregation, the linearity of Guinier plots at very small angles ($s < 1.3/R_g$) (Fig. 2S) suggests that the samples are monodisperse. The overall parameters from the SAXS data are summarized in Supp. Table S1, the experimental scattering data and the computed distance distribution functions of the wild-type and mutant β-DG are compared in Fig. 6C and 6D, respectively.

The excluded volume V_p and MM values for the β-DG^{WT} protein (respectively 41400 Å^3 and 24 kDa) were consistent with the values expected for dimeric species, considering that the theoretical MM of the monomer is 10.6 kDa and that the hydrated volume in Å^3 should be about twice of the MM in Da according to an empirical finding for globular proteins. Instead the p.Cys667Phe β-DG exhibited increased R_g (78.7 Å compared to 40.6 Å of the wild-type protein) and MM of ~160 kDa as determined by Guinier approximation, which is in agreement with the V_p of the particle (320000 Å^3).

Accordingly, the corresponding distance distribution functions, p(r), were markedly different. Even if both wild-type and p.Cys667Phe β-DG exhibited positively skewed profiles with tails at large distances characteristic of elongated particles, the comparison of p(r) functions (Fig. 6D) showed that the mutation of this residue led to a significant increase in the maximum dimension of the protein (i.e. D_{max} increased from 135±6 Å of the wild-type β-DG to 280±15 Å of p.Cys667Phe β-DG). This significant change in the maximum dimension of the protein, combined with a considerable increase in the corresponding R_g, confirms that this pathological missense mutation induces a change in the oligomerization state of β-DG.

It is interesting to note that the same set of measurements were performed in presence of an excess of reducing agent (10 mM DTT) without any significant change in the resulting scattering curves (data not shown). Therefore, the disulfide bonds reduction does not reverse the observed oligomerization process.

Oligomerization characteristics of p.Cys667Phe β-DG are likely to be associated to some level of tertiary structural organization

Beside the information on the association state and overall size parameters of biological macromolecules, SAXS experiments can also provide insights into their tertiary structure and enable to distinguish between ordered and disordered proteins (Receveur-Bréchot et al., 2006). In particular the Kratky plot is an extremely useful representation of the scattering intensity to quickly assess the globular nature of a polypeptide chain without any modeling. Moreover, the normalization performed to obtain dimensionless Kratky plots (Durand et al., 2010) allows to compare globular and extended proteins irrespective of their size, and thereby to infer the maximum amount of information from this representation. As expected from previous characterization of wild-type β-DG that resulted to be a natively unfolded protein (Bozzi et al., 2003), the corresponding curve (in blue in Fig. 5A) does not have a clear maximum and displays an initial monotonic increase in the lower *s*-region followed by a plateau, all the hallmarks of a fully disordered protein with very short elements of secondary structure (Receveur-Bréchot et al., 2006). Conversely dimensionless Kratky plot obtained for the mutant β-DG (in red in Fig. 7A) exhibits the bell-shape suggesting the presence of some residual structure (Receveur-Bréchot et al., 2006). Anyway the fact that this curve displays a maximum slightly shifted to an $s*R_g$ value larger than 1.75 (characteristic of folded compact globular proteins) point to some degree of residual flexibility (Durand et al., 2010).

In order to confirm that the observed differences in oligomerization behavior are associated to differences in oligomer folding as suggested by SAXS analysis, we performed DSF and limited proteolysis experiments.

In DSF spectroscopy, a hydrophobic probe (e.g., Sypro Orange) is added to the sample and the solution is then heated: the increasing hydrophobic environment enhances the quantum yield of the chromophore resulting in a dramatic increase of the fluorescent signal. The melting profile of wild-type β-DG, shown in Fig. 6B, indicates that the fluorescence signal was high even at the initial temperature, and failed to yield an observable unfolding transition as the temperature is raised. Assuming that wild-type β-DG is a natively unfolded protein, this high initial fluorescence is expected because non-globular folded proteins are characterized by extended open structures that expose hydrophobic residues (Phillips and de la Pena, 2011). The curve is typical of a protein that is poorly ordered and lacks a stable tertiary fold. The fluorophore readily binds the natively unfolded protein even at a low temperature and, as the temperature increases, is progressively quenched as the protein aggregates when is completely unfolded, masking the hydrophobic regions and excluding the dye. A significant change in profile was observed for pathological p.Cys667Phe β-DG. Although the initial fluorescence is still very high, the spectrum indicates a more complex transition model. Indeed fluorescence signal is still high at the initial temperature due to the presence of several exposed hydrophobic residues and starts lowering as the temperature increases, but a sigmoidal transition can be seen at higher temperatures, suggesting that p.Cys667Phe mutation may stabilize a more rigid fold, possibly introducing some degree of tertiary structures.

In line with these results, proteolysis experiments led to the fast and complete degradation of wild-type β-DG, implying that this protein is highly flexible and easily accessible for thermolysin (Fig. 6C) and for the additional five proteases that have been tested (Supp. Fig. S3). On the contrary, the single missense mutation p.Cys667Phe almost abolished

degradation by all the employed proteases (Fig. 6C and Supp. Fig. S3), likely inducing a more tightly packed conformation and thereby masking most of the cleavage sites.

Discussion

Hypoglycosylation of α-DG and the consequently weakening of the interactions between α-DG and its extracellular matrix binding partners, in particular laminins, are considered to be the hallmarks of several forms of primary and secondary dystroglycanopathies (Yoshida-Moriguchi and Campbell, 2015).

Our study provides the first molecular insight into a novel mechanism by which a missense mutation within the DG induces an altered folding and a pathological disulfide-associated oligomerization of the DG precursor, leading to its ER-retention and generating a severe skeletal muscle and central nervous system disorder. In fact, the homozygous mutation p.Cys667Phe was found in two siblings affected by a severe CMD and multicystic leukodystrophy (Geis et al., 2013). Immuno-histochemical staining of muscle biopsies showed the absence of glycosylated α-DG, although laminin-α2 was still localized at the sarcolemma. Currently, it is not clear yet if the primary DG defect caused by this mutation is a deficiency in α-DG trafficking and targeting to the plasma membrane or in its post-translational modification pathway, leading to hypoglycosylation and/or instability of the *core protein*.

The mutant DG precursor is entrapped in the ER and is targeted for degradation

Using transiently transfected Ebna-293 cells as heterologous cell expression system, we demonstrated that the p.Cys667Phe mutation, the murine counterpart of the human mutation, influences the correct processing of the DG precursor, inhibiting its post-translational cleavage into α- and β-DG (Fig. 1A). The mutated precursor is also likely to

have an altered glycosylation pattern, although still harbouring some N-acetyl-glucosamine residues, which allowed its successful sWGL pull-down (Fig. 1B). Interestingly, the p.Cys667Phe mutation might interfere with the action of oligosaccharyltransferase subunits that form mixed disulfide bonds with cysteines in substrate proteins to enhance N-glycosylation of nearby asparagine residues (Schultz et al., 2009; Mohd Yusuf et al., 2013). Several studies have shown that incomplete glycosylation may perturb the proper protein folding leading to ER stress and activation of the unfolded protein response (UPR) (Jayaprakash and Surolia 2017). Notably, p.Cys667Phe DG is mostly stuck in the ER and only traces of the precursor are able to reach the plasma membrane, as demonstrated by immunofluorescence staining and membrane-proteins enrichment (Figs. 2-4).

The p.Cys667Phe mutation hits the extracellular region of β-DG and it is predicted to disrupt a disulfide bond formed with the cysteine residue in position 711 in murine DG (Deyst et al., 1995; Watanabe et al., 2007; Sciandra et al., 2012). When Cys667 was mutated to alanine, the tertiary structure of DG precursor was altered and its post-translational cleavage was inhibited leading to the engulfment of the mutant in the ER (Watanabe et al., 2007; Sciandra et al., 2012). A similar behaviour was observed when the reciprocal Cys711 was mutated to alanine (Sciandra et al., 2012).

Misfolded proteins confined in the ER are targeted and translocated into the cytoplasm, where they undergo ubiquitin-dependent degradation *via* the proteasome, or autophagy/lysosomal degradation pathways (Cohen-Kaplan et al., 2016). Indeed, severe diseases might arise from mutations of proteins with an altered ER retention pattern due to their inability to undergo ER-associated degradation (ERAD) (Guerriero & Brodsky, 2012).

We show that the treatment of transfected cells with lactacystin, a potent proteasome inhibitor, increases the levels of different poly-ubiquitinated forms of the p.Cys667Phe DG mutant indicating that the mutant is indeed targeted for degradation (Fig. 5B). However, we have observed a paradoxical effect with lactacystin and p.Cys667Phe DG. Although lactacystin increases the level of DG^{WT}, preventing its degradation, significantly reduces the level of mutated DG (Fig. 5A). It was shown that lactacystin is a potent inducer of oxidative stress in the cells and triggers the formation of protein aggregates predominantly by intermolecular disulfide bridges (Demasi and Davies, 2003). From this result, we can speculate that lactacystin induces the formation of larger p.Cys667Phe DG oligomers that are not dispersed even by chemical reduction with β-mercaptoetanol and did not enter polyacrylamide gel (Fig. 5). Therefore, we can assume that the mutant DG is expressed as an uncleaved misfolded precursor that is prone to form oligomers that remain entrapped in the ER, where eventually would be degraded by ERAD. The autoproteolytic processing of the mutant DG precursor, that would liberate the two DG subunits (Esapa et al., 2003; Akhavan et al., 2008), might be impaired in this case by the instability of the mutant precursor and/or by the presence of such oligomers.

The p.Cys667Phe mutation induces the formation of DG homo-oligomers

To investigate the overall propensity of the mutant DG to form high molecular mass oligomers, we have expressed and purified the β-DG ectodomain carrying the p.Cys667Phe mutation as a recombinant protein for biochemical and biophysical studies *in vitro* (Di Stasio et al., 1999). It should be noted that this recombinant protein represents only the isolated ectodomain of β-DG, therefore lacking the C-terminal region of α-DG that would be still present in the unprocessed precursor within cells, and apparently in its wild-type form do not form an intra-molecular disulfide bridge between positions 667 and

711, displaying a largely unstructured fold (defined as natively unfolded) (Boffi et al., 2001; Bozzi et al., 2003). All considered, the recombinant ectodomain of β-DG represents the best available model to run biochemical experiments. Indeed, by a series a complementary techniques (SDS-PAGE under non-reducing conditions, native PAGE, gel filtration, DLS and SAXS measurements) it was demonstrated that the pathological p.Cys667Phe mutation promoted a disulfide-associated oligomerization process within the recombinant ectodomain of β-DG (Fig. 6). Considering that disulfide bonds reduction does not reverse p.Cys667Phe β-DG oligomerization, the inter-molecular disulfide bonds in the mutant β-DG are not crucial for the overall stabilization of the oligomeric assembly but are likely to be instead necessary for the initial oligomer formation. It is tempting to speculate that this inter-molecular covalent bond might provide a compact seed mediating the nucleation and further development of the oligomeric assembly. Indeed, several approaches (limited proteolysis together with DSF and SAXS analysis by Kratky plot) confirmed that p.Cys667Phe mutation alters β-DG overall conformation *in vitro*. These results suggest that the p.Cys667Phe mutation might enhance the stability of a sort of *initial dimeric folding nucleus* based on an intermolecular disulfide bond between Cys711. Hence, the p.Cys667Phe substitution may be regarded as a key residue to trigger intermolecular interactions leading to a higher-order assembly of the otherwise natively-unfolded wild-type β-DG protein with severe pathological consequences.

Implications for dystroglycanopathies

The results presented here suggest that the molecular basis of the disease induced by the p.Cys667Phe mutation would be a strong reduction of the amount of functional DG detected at the sarcolemma. Indeed, the mutant DG precursor is unable to mature in fully glycosylated α- and β-subunits, to correctly fold and to move on through its normal

pathway of intracellular trafficking. This would reflect in a significant reduction of properly glycosylated α-DG at the sarcolemma and would be in line with a range of muscular dystrophy phenotypes observed in other dystroglycanopathies (Michele et al., 2002). On the other hand, another striking pathological effect might originate intracellularly and might represent instead the first biochemical clue behind the complex observed pathology, which involves the central nervous system as well (Geis et al., 2013). In fact, the mutant DG precursor is retained in the ER where seems to be prone to undergo oligomerization process and where it could be eventually targeted for ubiquitin-mediated degradation. Interestingly, in a study based on the characterization of novel zebrafish mutants, it was already hypothesized that dystroglycanopathies may also arise from the impairment of DG secretion resulting in an acute ER stress (Lin et al., 2011).

The primary dystroglycanopathies so far identified are thought to be caused by mutations that influence the interaction between α-DG and LARGE (Hara et al., 2011; Dong et al., 2015). In particular, the p.Thr192Met mutation, identified in a LGMD patient, and p.Val74Ile and p.Asp111Asn mutations identified in a mild form of muscular dystrophy, are located within the N-terminal domain of α-DG that was proposed to be important for the interaction between LARGE and α-DG (Kanagawa et al., 2004). Therefore, p.Cys667Phe/ p.Cys669Phe is the first pathological mutation found within the β-DG subunit that strongly alters the post-translational processing of the DG thus inducing oligomerization and ER-retention of the mutant DG precursor.

Different genetic diseases, including muscular dystrophies, are characterized by ER-retention of misfolded mutant proteins that are recognized by the ER quality control machinery and degraded by the ubiquitin-proteasome system. In particular, different LGMDs, caused by mutations in sarcoglycans as well as CMDs, caused by mutations in

the fukutin-related-protein (FKRP, MIM# 606596) (Esapa et al., 2005; Bartoli et al., 2008; Soheli et al., 2012; Bianchini et al., 2014). In addition, Duchenne muscular dystrophy, which is most typically caused by mutations that lead to loss of dystrophin expression, is also associated to missense mutations within the actin-binding domain of dystrophin that lead to protein instability and aggregation (Singh et al., 2010; Henderson et al., 2010).

The p.Cys669Phe patient is affected by CMD characterized by severe central nervous system defects associated with extended bilateral multicystic white matter disease (Geis et al., 2013). The clinical phenotype induced by p.Cys667Phe/ p.Cys669Phe seem to overlap with the brain clinical features observed in patients affected by megalencephalic leukoencephalopathy with subcortical cysts (MLC1, MIM# 604004) (Van der Knaap et al., 1995). MLC1 is due to mutations in *MLC1* gene (MIM# 605908), which encodes for an oligomeric membrane protein highly expressed in astrocytes, where it is thought to regulate ions and water homeostasis (Brignone et al., 2015). In addition, MLC1 has been shown to interact with the DGC (Boor et al., 2007; Ambrosini et al., 2008). Interestingly, the molecular bases of MCL1 might be similar to those we propose for p.Cys667Phe dystroglycanopathy. Indeed, mutations in MLC1 induce protein misfolding, reduced plasma membrane targeting/expression and ER retention of the mutant MLC1 (Xie et al., 2012). Moreover, agrin and α-DG show an altered distribution in the brain of patients affected by MLC (Boor et al., 2007). A feature of the DGC is that mutations affecting one of its components often lead to destabilization of the entire complex with reduced or altered expression of other members of the complex. It will be interesting to unravel whether the leukodystrophy phenotype observed in the p.Cys669Phe patients is primarily

due to the altered expression of mutant DG or to an overall disassembling of the DGC/MLC1 molecular scaffold.

Is the increased accumulation of misfolded/aggregated protein in the ER in itself contributing to the observed phenotype? At present, this is not known but it may be interesting to consider that an enhanced protein targeting and degradation is currently considered as a promising therapeutic tool (Collins et al., 2017). On the other hand, although with controversial outcomes especially in oncotherapy (Manasanch and Orlowski, 2017), pharmacological inhibition of proteasome had been proposed as a possible strategy for rescuing membrane localization of mutated and partly unstable proteins. The general idea behind such therapeutic strategies is that some of the misfolded proteins, if able to escape the cell's quality-control system, might still be functional if targeted to the correct cellular location. This trend was demonstrated for sarcoglycans (Gastaldello et al., 2008), for laminin-α2 (Carmignac et al., 2011) as well as for the most common mutant of the cystic fibrosis transmembrane conductance regulator gene (*CFTR*, MIM# 602421), Phe508DEL, among others (Cheng et al., 1990). However, our data might suggest that inhibition of proteasome-mediated degradation of p.Cys667Phe DG is not likely to be an effective therapy for treating the symptoms of the associated dystroglycanopathy. In fact, lactacystin induces the formation of higher molecular mass protein oligomers that end up stuck in ER where they would be likely submitted to extensive degradation processes. Additional studies will be required to elucidate which molecular pathways are exactly activated in order to degrade this mutated DG and possibly to identify novel targets for therapy.

Acknowledgements

This work was supported by the Association Française contre les Myopathies (grant n.20009 to AB). Confocal imaging data were obtained at the LABCEMI (Laboratorio Centralizzato di Microscopia Ottica ed Elettronica) of the Università Cattolica del S. Cuore di Roma (Italy).

Disclosure statement

The authors declare that they have no conflict of interest.

References

Akhavan A, Crivelli SN, Singh M, Lingappa VR Muschler JL. 2008. SEA domain proteolysis determines the functional composition of dystroglycan. FASEB J 22, 612-621.

Ambrosini E, Serafini B, Lanciotti A, Tosini F, Scialpi F, Psaila R, Raggi C, Di Girolamo F, Petrucci TC, Aloisi F. 2008. Biochemical characterization of MLC1 protein in astrocytes and its association with the dystrophin-glycoprotein complex. Mol Cell Neurosci 37: 480-493.

Bartoli M, Gicquel E, Barrault L, Soheili T, Malissen M, Malissen B, Vincent-Lacaze N, Perez N, Udd B, Danos O, Richard I. 2008. Mannosidase I inhibition rescues the human α-sarcoglycan R77C recurrent mutation. Hum Mol Genet 17:1214-1221.

Bassat E, Mutlak YE, Genzelinakh A, Shadrin IY, Baruch-Umansky K, Yifa O, Kain D, Rajchman D, Leach J, Bassat DR, Udi Y, Sarig R, Sagi I, Martin JF, Bursac N, Cohen S, Tzahor E. 2017. The extracellular matrix protein agrin promotes heart regeneration in mice. Nature 547: 179-184.

Bianchini E, Fanin M, Mamchaoui K, Betto R, Sandonà D. 2014.Unveiling the degradative route of the V247M α-sarcoglycan mutant responsible for LGMD-2D. Hum Mol Genet 23:3746-3758.

Blanchet CE, Spilotros A, Schwemmer F, Graewert MA, Kikhney A, Jeffries CM, Franke D, Mark D, Zengerle R, Cipriani F, Fiedler S, Roessle M, Svergun DI. 2015 Versatile sample environments and automation for biological solution X-ray scattering experiments at the P12 beamline (PETRA III, DESY). J Appl Crystallogr 48: 431-443.

Boor R, Jacobs J, Hinzmann A, Bauermann T, Scherg M, Boor S, Vucurevic G, Pfleiderer C, Kutschke G, Stoeter P. 2007. Combined spike-related functional MRI and multiple source analysis in the non-invasive spike localization of benign rolandic epilepsy. Clin Neurophysiol 118: 901-909

Boffi A, Bozzi M, Sciandra F, Woellner C, Bigotti MG, Ilari A, Brancaccio A. 2001. Plasticity of secondary structure in the N-terminal region of β-dystroglycan. Biochim Biophys Acta 1546: 114-121.

Bozzi M, Bianchi M, Sciandra F, Paci M, Giardina B, Brancaccio A, Cicero DO. 2003. Structural characterization by NMR of the natively unfolded extracellular domain of β-dystroglycan: toward the identification of the binding epitope for α-dystroglycan. Biochemistry 42:13717-13724.

Bozzi M, Morlacchi S, Bigotti MG, Sciandra F, Brancaccio A. 2009. Functional diversity of dystroglycan. Matrix Biol 28, 179-187.

Bozzi M, Cassetta A, Covaceuszach S, Bigotti MG, Bannister S, Hübner W, Sciandra F, Lamba D, Brancaccio A. 2015. The structure of the T190M mutant of murine α-dystroglycan at high resolution: insight into the molecular basis of a primary dystroglycanopathy. PLoS One 10, e0124277.

Brancaccio A, Schulthess T, Gesemann M, Engel J.1997. The N-terminal region of α-dystroglycan is an autonomous globular domain. Eur J Biochem 246, 166-172.

Briggs DC, Yoshida-Moriguchi T, Zheng T, Venzke D, Anderson ME, Strazzulli A, Moracci M, Yu L, Hohenester E, Campbell KP. 2016. Structural basis of laminin binding to the LARGE glycans on dystroglycan. Nature Chem Biol 12: 810-814.

Carmignac V, Quéré R, Durbeej M. 2011. Proteasome inhibition improves the muscle of laminin α2 chain-deficient mice. Hum Mol Genet 20:541-552.

Cheng SH, Gregory RJ, Marshall J, Paul S, Souza DW, White GA, O'Riordan CR, Smith AE.1990. Defective intracellular transport and processing of CFTR is the molecular basis of most cystic fibrosis. Cell 63:827-834.

Cohen-Kaplan V, Livneh I, Avni N, Cohen-Rosenzweig C, Ciechanover A. 2016. The ubiquitin-proteasome system and autophagy: coordinated and independent activities. Int J Biochem Cell Biol 79: 403-418.

Collins I, Wang H, Caldwell JJ, Chopra R. 2017. Chemical approaches to targeted protein degradation through modulation of the ubiquitin-proteasome pathway. Biochem J 474: 1127-1147.

Colognato H, Winkelmann DA, Yurchenco PD. 1999. Laminin polymerization induces a receptor-cytoskeleton network. J Cell Biol 145: 619-631.

Covaceuszach S, Bozzi M, Bigotti MG, Sciandra F, Konarev PV, Brancaccio A, Cassetta A. 2017a. Structural flexibility of human α-dystroglycan. FEBS Open Bio 7; 1064-1077.

Covaceuszach S, Bozzi M, Bigotti MG, Sciandra F, Konarev PV, Brancaccio A, Cassetta A. 2017b. The effect of the pathological V72I, D109N and T190M missense mutations on the molecular structure of α-dystroglycan. PLoS One 12, e0186110.

Demasi M, Davies KJ. 2003. Proteasome inhibitors induce intracellular protein aggregation and cell death by an oxygen-dependent mechanism. FEBS Lett 542: 89-94.

Deyst KA, Bowe MA, Leszyk JD, Fallon JR. 1995. The α-dystroglycan-β-dystroglycan complex. J Biol Chem 270: 25956-25959.

Di Stasio E, Sciandra F, Maras B, Di Tommaso F, Petruci TC, Giardina B, Brancaccio A. 1999. Structural and functional analysis of the N-terminal extracellular region of β-dystroglycan. Biochem Biophys Res Commun: 266: 274-278

Dong M, Noguchi S, Endo Y, Hayashi YK, Yoshida S, Nonaka I, Nishino I. 2015. DAG1 mutations associated with asymptomatic hyperCKemia and hypoglycosylation of α-dystroglycan. Neurology 84:273–279.

Durand D, Vivès C, Cannella D, Pérez J, Pebay-Peyroula E, Vachette P, Fieschi F. 2010 NADPH oxidase activator p67phox behaves in solution as a multidomain protein with semi-flexible linkers. J Struct Biol 169, 45-53.

Esapa CT, Bentham GRB, Schröder JE, Kröger S, Blake DJ. 2003. The effects of post-translational processing on dystroglycan synthesis and trafficking. FEBS Lett 555: 209-216.

Esapa CT, McIlhinney RA, Blake DJ. 2005. Fukutin-related protein mutations that cause congenital muscular dystrophy result in ER-retention of the mutant protein in cultured cells. Hum Mol Genet 14: 295-305.

Gastaldello S, D'Angelo S, Franzoso S, Fanin M, Angelini C, Betto R, Sandonà D. 2008. Inhibition of proteasome activity promotes the correct localization of disease-causing α-sarcoglycan mutants in HEK-293 cells constitutively expressing β-, γ-, and δ-sarcoglycan. Am J Pathol 173:170-181.

Geis T, Marquard K, Rödl T, Reihle C, Schirmer S, von Kalle T, Bornemann A, Hehr U, Blankenburg M. 2013. Homozygous dystroglycan mutation associated with a novel

muscle-eye-brain disease-like phenotype with multicystic leucodystrophy. Neurogenetics 14: 205-213.

Guerriero CJ and Brodsky JL. 2012. The delicate balance between secreted protein folding and endoplasmic reticulum-associated degradation in human physiology. Physiol Rev 92: 537-576.

Guinier A. 1939. La diffraction des rayons X aux tres petits angles: applications a l'etude de phenomenes ultramicroscopiques. Ann Phys Paris 12, 161-237.

Hara Y, Balci-Hayta B, Yoshida-Moriguchi T, Kanagawa M, Beltrán-Valero de Bernabé D, Gündeşli H, Willer T, Satz JS, Crawford RW, Burden SJ, Kunz S, Oldstone MB, Accardi A, Talim B, Muntoni F, Topaloğlu H, Dinçer P, Campbell KP. 2011. A dystroglycan mutation associated with limb-girdle muscular dystrophy. N Engl J Med 364: 939-946.

Henderson DM, Lee A, Ervasti JM. 2010. Disease-causing missense mutations in actin binding domain 1 of dystrophin induce thermodynamic instability and protein aggregation. Proc Natl Acad Sci U S A 107:9632-963.

Ibraghimov-Beskrovnaya O, Ervasti JM, Leveille CJ, Slaughter CA, Sernett SW, Campbell KP. 1992. Primary structure of dystrophin-associated glycoproteins linking dystrophin to the extracellular matrix. Nature 35:696-702.

Jayaprakash NG, Surolia A. 2017. Role of glycosylation in nucleating protein folding and stability. Biochem J. 474: 2333-2347.

Jayasinha V, Nguyen HH, Xia B, Kammesheidt A, Hoyte K, Martin PT. 2003. Inhibition of dystroglycan cleavage causes muscular dystrophy in transgenic mice. Neuromuscul Disord 13:365-375.

Kanagawa M, Kobayashi K, Tajiri M, Manya H, Kuga A, Yamaguchi Y, Akasaka-Manya K, Furukawa J, Mizuno M, Kawakami H, Shinohara Y, Wada Y, Endo T, Toda T. 2016. Identification of a post-translational modification with ribitol-Phosphate and its defect in muscular dystrophy. Cell Rep 14:2209-2223.

Kanagawa M, Saito F, Kunz S, Yoshida-Moriguchi T, Barresi R, Kobayashi YM, Muschler J, Dumanski JP, Michele DE, Oldstone MB, Campbell KP. 2004. Molecular recognition by LARGE is essential for expression of functional dystroglycan. Cell 25:953-964.

Konarev PV, Volkov VV, Sokolova AV, Koch MHJ, Svergun DI. 2003 *PRIMUS*: a Windows PC-based system for small-angle scattering data analysis. J Appl Crystallogr 36, 1277-1282.

Lin YY, White RJ, Torelli S, Cirak S, Muntoni F, Stemple DL. 2011. Zebrafish fukutin family proteins link the unfolded protein response with dystroglycanopathies. Hum Mol Genet. 20: 1763-1775.

Manasanch EE, Orlowski RZ. 2017. Proteasome inhibitors in cancer therapy. Nat Rev Clin Oncol 14:417-433.

Michele DE, Barresi R, Kanagawa M, Saito F,Cohn RD, Satz JS, Dollar J, Nishino I, Kelley RI, Somer H, Straub V, Mathews KD, Moore SA, Campbell KP. 2002. Post-

translational disruption of dystroglycan-ligand interactions in congenital muscular dystrophies. Nature 418:417-421.

Mohd Yusuf SN, Bailey UM, Tan NY, Jamaluddin MF, Schulz BL. 2013. Mixed disulfide formation in vitro between a glycoprotein substrate and yeast oligosaccharyltransferase subunits Ost3p and Ost6p. Biochem Biophys Res Commun. 432: 438-443.

Moore CJ, Winder SJ. 2012. The inside and out of dystroglycan post-translational modification. Neuromuscul Disord 22:959-965.

Morikawa Y, Heallen T, Leach J, Xiao J, Martin JF. 2017. Dystrophin glycoprotein complex sequesters Yap to inhibit cardiomyocyte proliferation. Nature 547: 227-231.

Morlacchi S, Sciandra F, Bigotti MG, Bozzi M, Hübner W, Galtieri A, Giardina B, Brancaccio A. 2012. Insertion of a myc-tag within α-dystroglycan domains improves its biochemical and microscopic detection. BMC Biochem 13:14.

Palmieri V, Bozzi M, Signorino G, Papi M, De Spirito M, Brancaccio A, Maulucci G, Sciandra F. 2017. α-Dystroglycan hypoglycosylation affects cell migration by influencing β-dystroglycan membrane clustering and filopodia length: a multiscale confocal microscopy analysis. Biochim Biophys Acta 1863: 2182-2191.

Petoukhov MV, Franke D, Shkumatov AV, Tria G, Kikhney AG, Gajda M, Gorba C, Mertens HDT, Konarev PV, Svergun DI. 2012 New developments in the ATSAS program package for small-angle scattering data analysis. J Appl Cryst 45: 342-350.

Phillips K and de la Pena AH 2011 The combined use of the Thermofluor assay and ThermoQ analytical software for the determination of protein stability and buffer

optimization as an aid in protein crystallization. Curr. Protoc. Mol. Biol. Chapter 10, Unit 10.28.

Porod, G. 1982 In: Small Angle X-ray Scattering. Academic Press, p 17-51.

Receveur-Bréchot V, Bourhis JM, Uversky VN, Canar, B, Longhi S. 2006 Assessing protein disorder and induced folding. Proteins 62: 24-45.

Riemersma M, Mandel H, van Beusekom E, Gazzoli I, Roscioli T, Eran A, Gershoni-Baruch R, Gershoni M, Pietrokovski S, Vissers LE, Lefeber DJ, Willemsen MA, Wevers RA, van Bokhoven H. 2015. Absence of α- and β-dystroglycan is associated with Walker-Warburg syndrome. Neurology 84: 2177-82.

Russo K, Di Stasio E, Macchia G, Rosa G, Brancaccio A, Petrucci TC. 2000. Characterization of the β-dystroglycan-growth factor receptor 2 (Grb2) interaction. Biochem Biophys Res Commun 274: 93-98.

Schulz BL, Stirnimann CU, Grimshaw JP, Brozzo MS, Fritsch F, Mohorko E, Capitani G, Glockshuber R, Grütter MG, Aebi M. 2009. Oxidoreductase activity of oligosaccharyltransferase subunits Ost3p and Ost6p defines site-specific glycosylation efficiency. Proc Natl Acad Sci U S A. 106: 11061-11066.

Sciandra F, Schneider M, Giardina B, Baumgartner S, Petrucci TC, Brancaccio A. 2001. Identification of the β-dystroglycan binding epitope within the C-terminal region of α-dystroglycan. Eur J Biochem 268: 4590-4597.

Sciandra F, Angelucci E, Altieri F, Ricci D, Hübner W, Petrucci TC, Giardina B, Brancaccio A, Bozzi M. 2012. Dystroglycan is associated to the disulfide isomerase ERp57. Exp Cell Res 318: 2460-2469.

Singh SM, Kongari N, Cabello-Villegas J, Mallela KM. 2010. Missense mutations in dystrophin that trigger muscular dystrophy decrease protein stability and lead to cross-β aggregates. Proc Natl Acad Sci U S A 107: 15069-15074.

Soheili T, Gicquel E, Poupiot J, N'Guyen L, Le Roy F, Bartoli M, Richard I. 2012. Rescue of sarcoglycan mutations by inhibition of endoplasmic reticulum quality control is associated with minimal structural modifications. Hum Mutat 33: 429-39.

Spence HJ, Dhillon AS, James M, Winder SJ. 2004. Dystroglycan, a scaffold for the ERK-MAP kinase cascade. Embo Rep 5:484-489.

Svergun DI. 1992 Determination of the regularization parameter in indirect-transform methods using perceptual criteria. J. Appl. Crystallogr. 25: 495-503.

Watanabe N, Sasaoka T, Noguchi S, Nishino I, Tanaka T. 2007. Cys669-Cys713 disulfide bridge formation is a key to dystroglycan cleavage and subunit association. Genes Cells 12: 75-88.

Willer T, Inamori K, Venzke D, Harvey C, Morgensen G, Hara Y, Beltrán Valero de Bernabé D, Yu L, Wright KM, Campbell KP. 2014. The glucuronyltransferase B4GAT1 is required for initiation of LARGE-mediated α-dystroglycan functional glycosylation. Elife 10.7554/eLife.03941.

Yoshida-Moriguchi T, Campbell KP. 2015. Matriglycan: a novel polysaccharide that links dystroglycan to the basement membrane. Glycobiology 25:702-13.

Figure legends

Fig. 1. A) p.Cys667Phe mutation inhibits DG precursor cleavage: total protein extracts of Ebna-293 cells transfected with wild-type, p.Ser652Ala, and p.Cys667Phe DG-GFP were analysed by Western blot. Nitrocellulose membranes were probed with anti β-DG 43-DAG antibody and with anti-tubulin antibody used as loading control. For wild-type DG, the band at about 70 kDa (arrow) refers to β-DG-GFP whilst for p.Cys667Phe DG, the α/β DG precursor is observed similarly to p.Ser652Ala DG used for control at about 135 kDa (asterisk). Lower bands are present in all the samples that are produced by a degradation taking place within the ectodomain of β-DG (Bozzi et al., 2009). **B) p.Cys667Phe DG harbours N-acetylglucosamine residues:** total protein extracts of Ebna-293 cells transfected with wild-type , p.Ser652Ala, and p.Cys667Phe DG-GFP were incubated with succynilated-Wheat Germ Lectin (sWGL) and bound proteins were eluted with N-acetylglucosamine for Western blot analysis. Nitrocellulose was probed with anti β-DG 43-DAG antibody. * indicates the DG precursor.

FIG 1

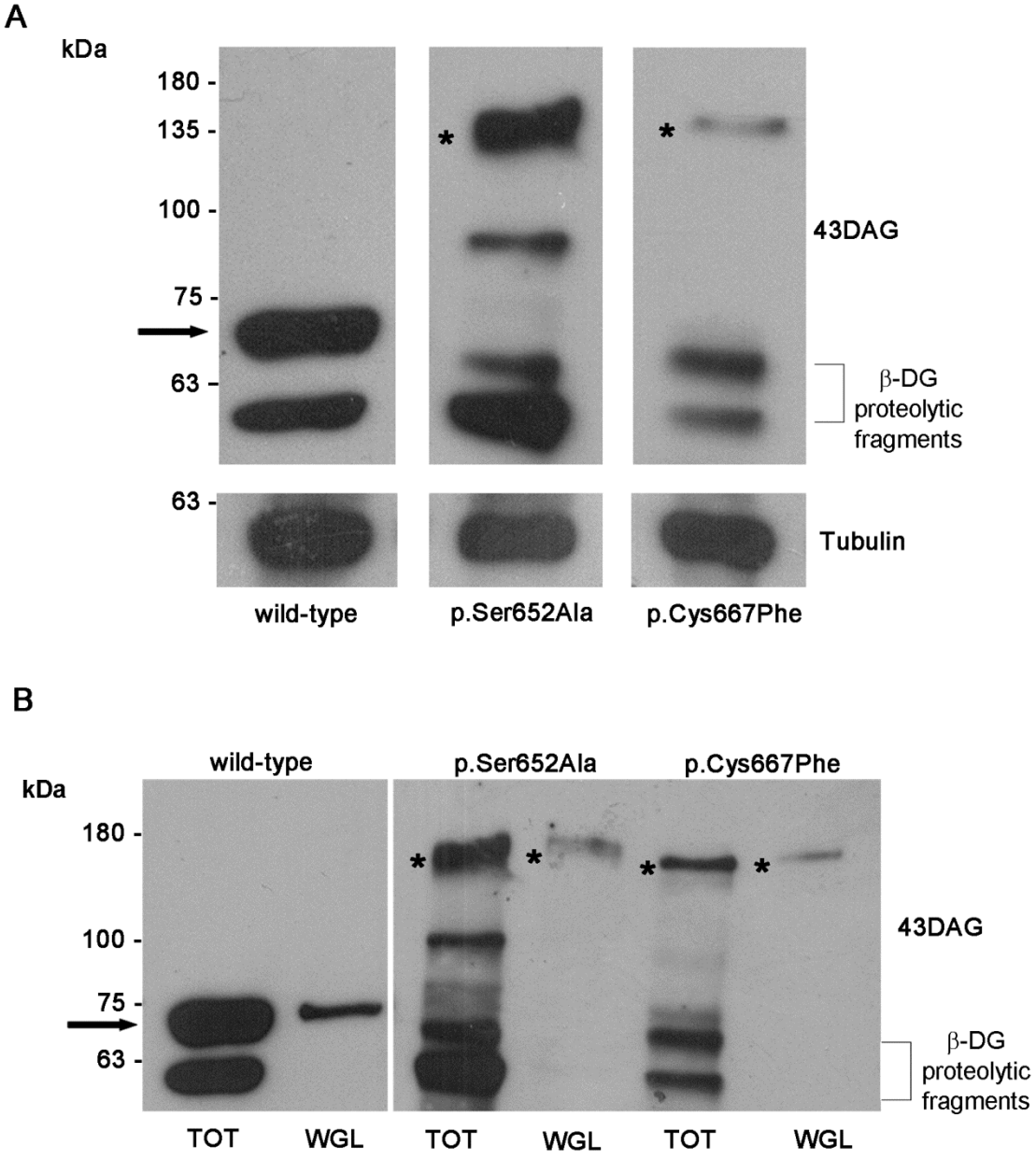

Fig. 2. p.Cys667Phe is mostly retained in the ER: Ebna-293 cells transfected with wild-type DG-GFP and p.Cys667Phe DG-GFP were fixed and used for surface or intracellular immunofluorescence analysis. In **A)** Anti-myc antibody was used to labell α-DG whilst the intrinsic fluorescent signal of GFP reported β-DG localization. Surface staining showed the membrane localization of α- and β-DG in cells expressing wild-type DG. In contrast, p.Cys667Phe DG fails to reach the cell surface as indicated by the spare anti-myc antibody signals and by the reticular signals of GFP inside the cells. Intracellular staining, confirmed the membrane localization of wild-type DG and the intracellular retention of p.Cys667Phe DG whose reticular distribution was recognized also by the anti-myc antibody. Scale bar: 20μm. **B)** Anti Erp57 antibody was used to labell ER in permeable transfected cells. While the wild-type DG is localized at the plasma membrane and in some large dots in the cytoplasm, the mutated DG is mainly entrapped in the ER. Nuclei were counterstained with DAPI. Scale bar: 20μm.

FIG 2A

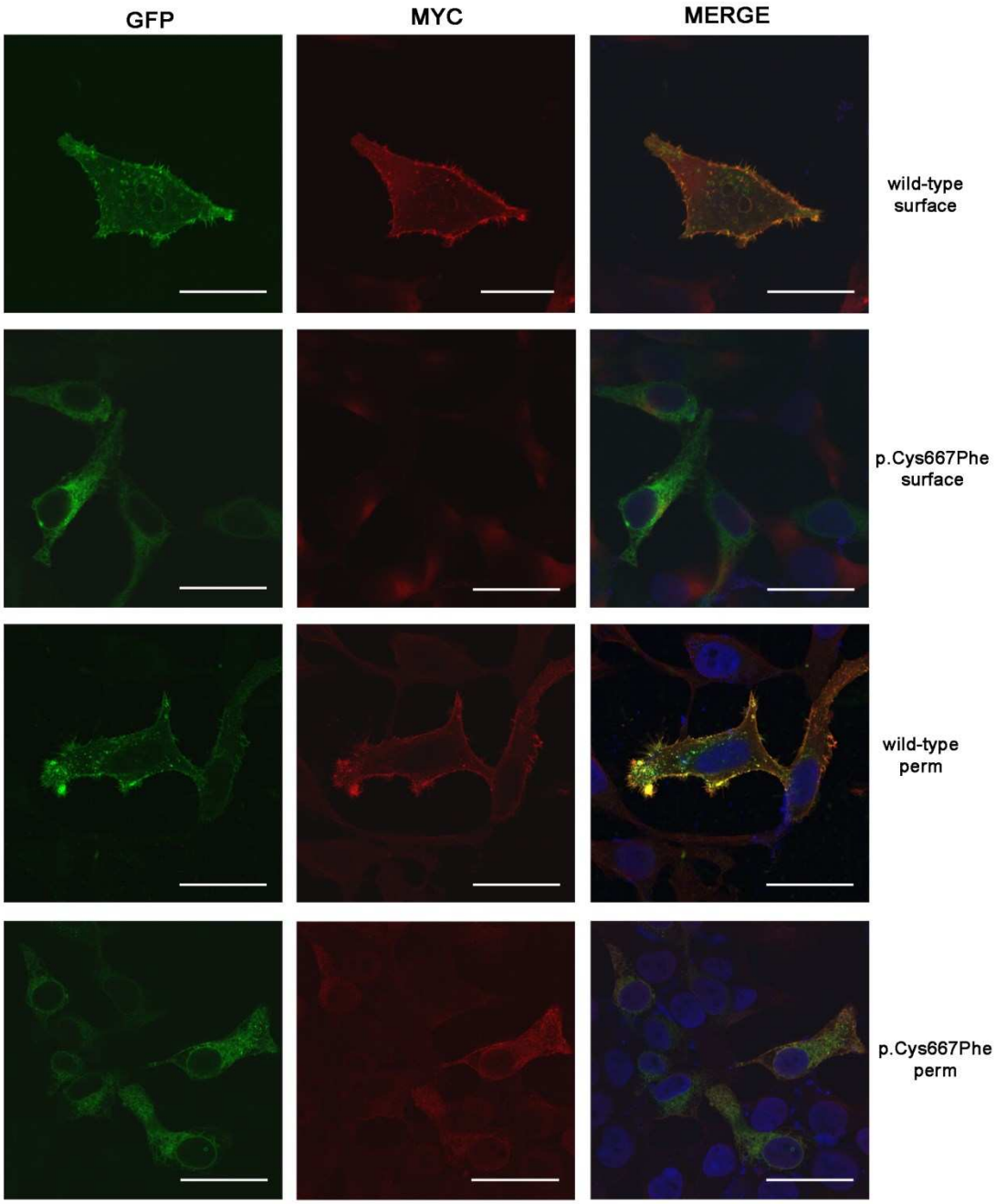

FIG 2B

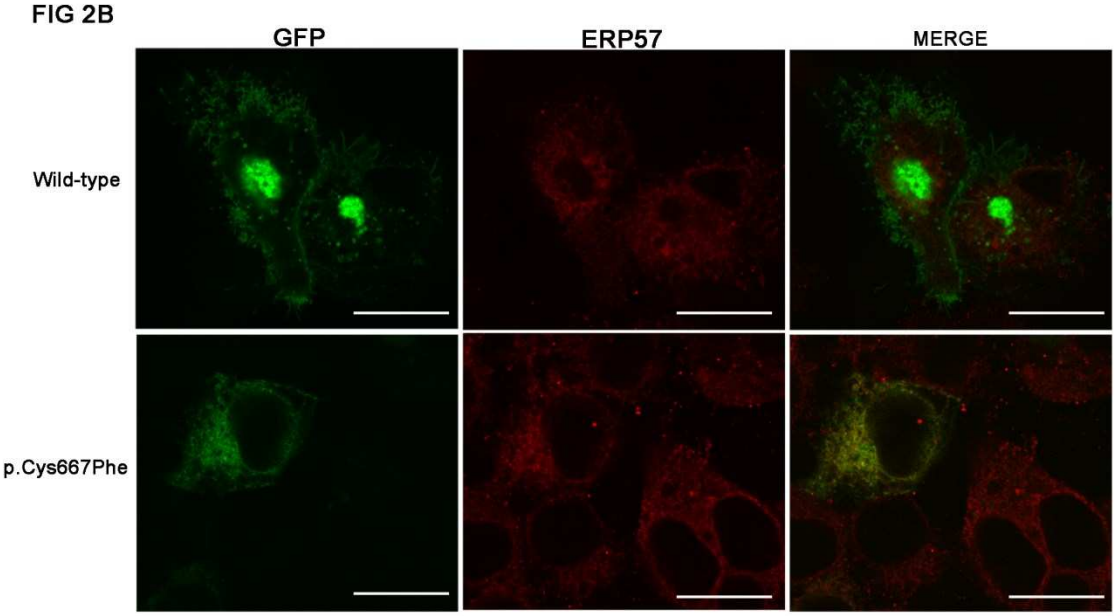

Fig. 3. Super-resolution 3D Structured Illumination Microscopy images of wild-type DG and p.Cys667Phe DG transiently expressed in U2OS cells. The mutant accumulates mostly in the ER and reaches rarely the plasma membrane. The top row shows a cell expressing wild-type DG-GFP, the bottom row the mutant p.Cys667Phe DG-GFP. The individual images for DAPI staining of the nucleus, the DG GFP signal and the ER-Tracker Red ER and mitochondrial staining are shown as well as an overlay of these three channels (blue, green, red respectively). The images represent the maximum intensity projection of 4 z slices corresponding to 500nm thickness.

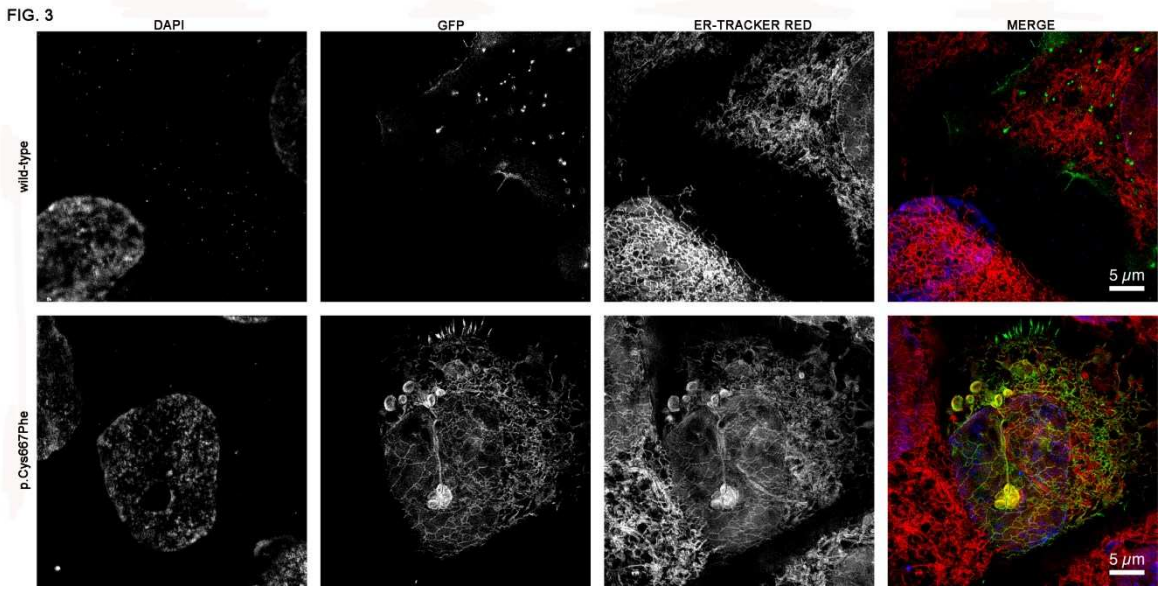

Fig. 4. p.Cys667Phe DG is poorly targeted to the plasma membrane. Ebna-293 cells were transfected with wild-type , p.Ser652Ala, and p.Cys667Phe DG-GFP and, following cell surface biotinylation, membrane proteins were precipitated with NeutrAvidin Agarose beads and analysed with Western blot. Nitrocellulose was probed with anti β-DG 43-DAG antibody and with anti-calnexin antibody as negative control. For wild-type DG, the band at about 70 kDa (arrow) refers to β-DG-GFP that is enriched in the plasma membrane proteins fraction (Memb.) compared to the total (TOT). For p.Cys667Phe DG, the α/β DG precursor present in the total cell extracts (TOT) (asterisk) is diminished in the plasma membrane proteins fraction (Memb.). The 43kDa band corresponds to the endogenous β-DG (e). The area of wild-type DG and p.Cys667Phe DG bands were measured with ImageJ software and were normalized to endogenous DG. The error bars show the Standard Error of Mean (SEM) from four independent experiments (* $p<0,05$).

FIG 4

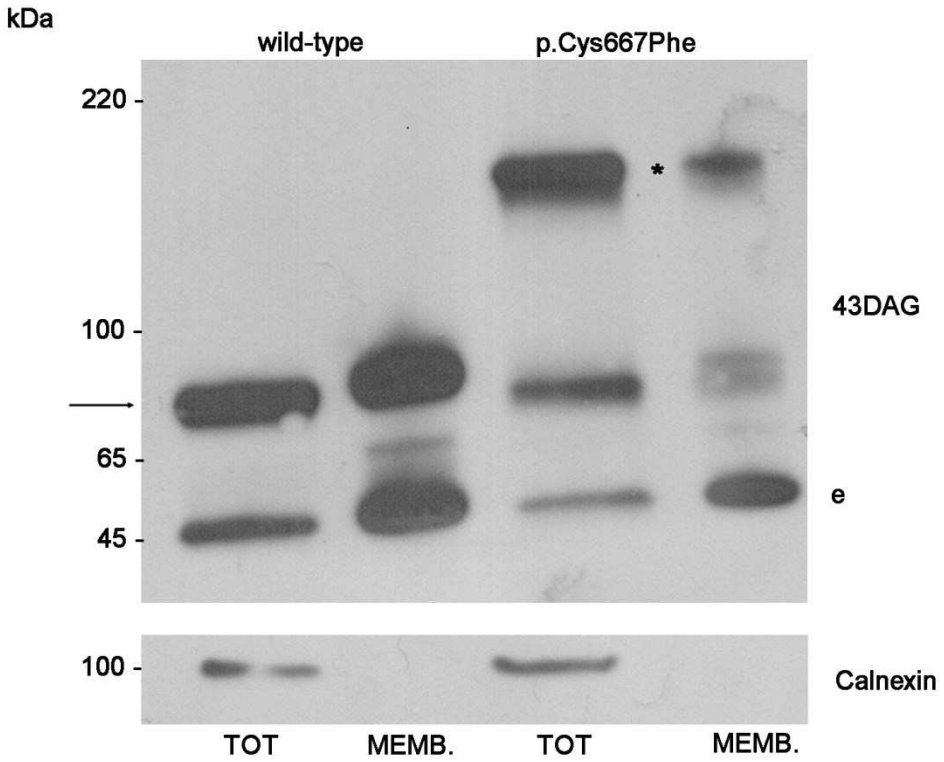

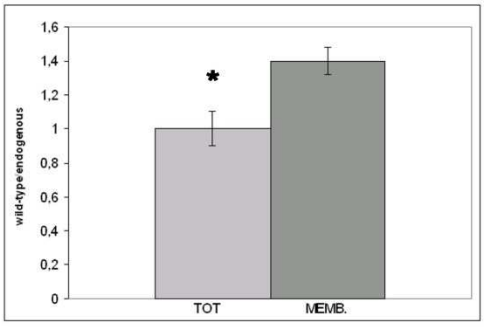

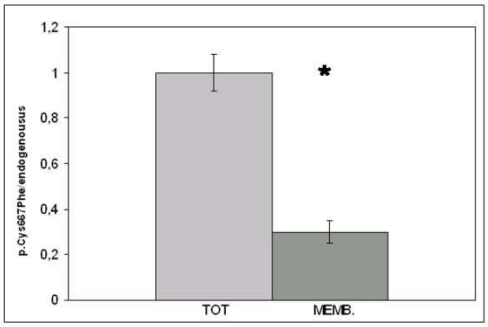

Fig. 5. Proteasome inhibitor lactacystin increases the poly-ubiquitination of DG. A) Western blot analysis of total protein extracts (20μg) from Ebna-293-cells transfected with wild-type DG-GFP and p.Cys667Phe DG-GFP and treated with (+) or without (-) the proteasome inhibitor lactacystin. Anti-43DAG was used to stain β-DG and anti-tubulin as loading control. Treatment with lactacystin increased the level of wild-type DG as well as that of the endogenous DG (e) whilst decreased the level of p.Cys667Phe DG precursor (asterisk). The area of wild-type DG and p.Cys667Phe DG bands were measured with ImageJ software and were normalized to tubulin. The error bars show the SEM from four independent experiments (*p<0,05). **B)** Total protein extracts from Ebna-293 cells transfected with wild-type DG and p.Cys667Phe DG and treated with (+) or without (-) lactacystin, were immunoprecipitated with anti-GFP agarose beads and the eluted sample analysed by Western blot. Nitrocellulose was incubated with anti-ubiquitin antibody. In lactacystin (+) treated cells an increase of the amount of polyubiquitinated wild-type DG and p.Cys667Phe DG was observed compared to absence of lactacystin (-).

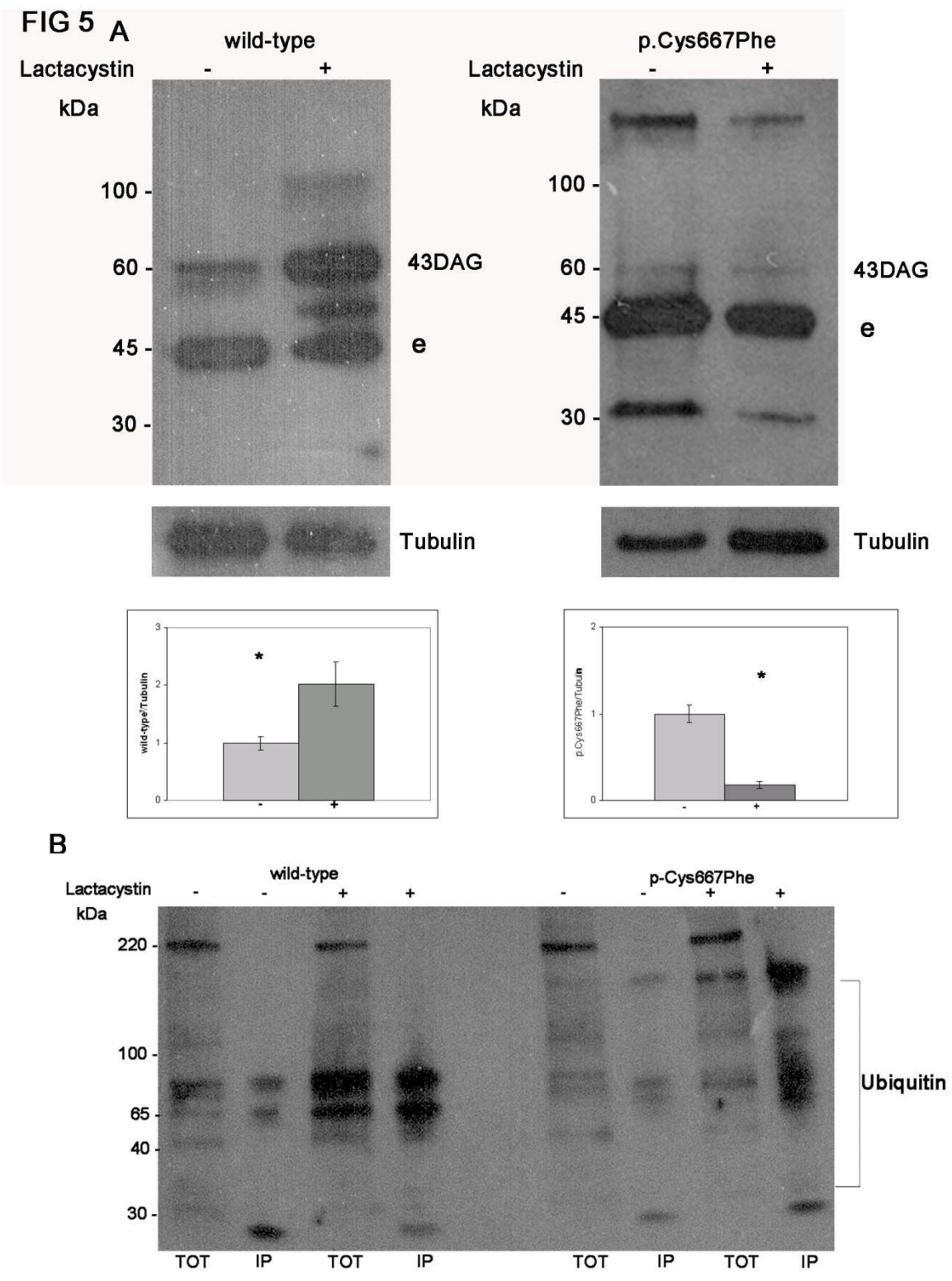

Fig. 6. Oligomerization states of wild-type β-DG and p.cys667Phe β-DG. (A) Reducing and non-reducing SDS-PAGE % of wild-type β-DG and p.Cys667Phe β-DG. **(B)** Analytical gel filtration analysis of wild-type β-DG and p.Cys667Phe β-DG, in 20 mM Tris, 150 mM NaCl, at pH 7.5; fractions corresponding to the main peaks have been checked by 15% SDS PAGE (see the insert). **(C)** Experimental SAXS patterns (the plots display the logarithm of the scattering intensity as a function of momentum transfer $s = [4\pi\sin(\theta/2)]/\lambda$ ($Å^{-1}$), where θ is the scattering angle and λ is the X-ray wavelength) of wild-type β-DG and p.Cys667Phe β-DG and **(D)** derived distance distribution functions of wild-type β-DG and p.Cys667Phe β-DG.

FIG. 6

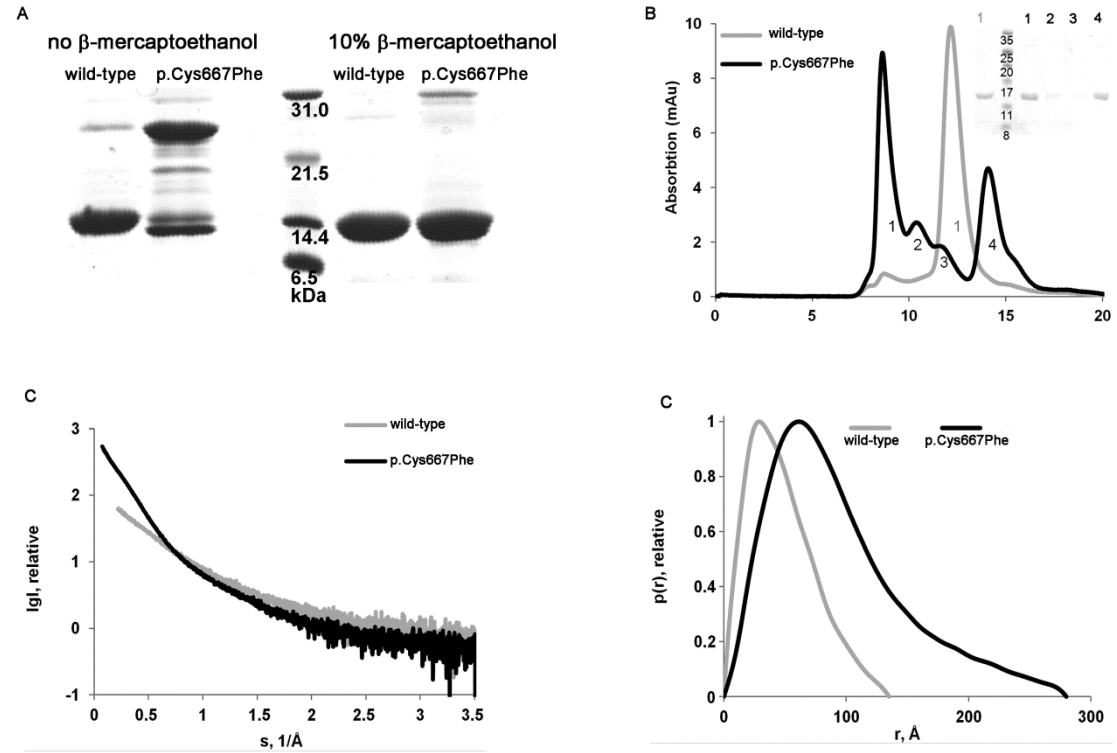

Fig. 7. p.Cys667Phe mutation induces some degree of tertiary structures in β-DG. A) Dimensionless Kratky plots derived from SAXS measurements of wild-type β-DG and p.cys667Phe β-DG; **B**) Thermal denaturation assay using DSF of wild-type β-DG and p.cys667Phe β-DG with SYPRO© dye. Experiments were performed in triplicate. **C**) Protease digestion of wild-type β-DG and p.cys667Phe β-DG by thermolysin, for 1, 5, 10, 20, 40 and 60 min. Undigested protein served as the zero time point (0).